

# Competition of superconducting pairing symmetries in $\text{La}_3\text{Ni}_2\text{O}_7$

Han-Xiang Xu,<sup>1</sup> Yue Xie,<sup>1,2</sup> Daniel Guterding,<sup>3</sup> and Zhijun Wang<sup>1,2</sup>

<sup>1</sup>*Beijing National Laboratory for Condensed Matter Physics,*

*Institute of Physics, Chinese Academy of Sciences, Beijing 100190, China*

<sup>2</sup>*School of Physical Sciences, University of Chinese Academy of Sciences, Beijing 100049, China*

<sup>3</sup>*Technische Hochschule Brandenburg, Magdeburger Straße 50, 14770 Brandenburg an der Havel, Germany*

(Dated: January 10, 2025)

The recent discovery of superconductivity in the bilayer Ruddlesden-Popper nickelate  $\text{La}_3\text{Ni}_2\text{O}_7$  under high pressure has generated much interest in the superconducting pairing mechanism of nickelates. Various theoretical approaches have been applied to the study of superconductivity in  $\text{La}_3\text{Ni}_2\text{O}_7$ , but lead to a number of contradicting results. We argue that different superconducting states in  $\text{La}_3\text{Ni}_2\text{O}_7$  are in close competition and at the same time particularly sensitive to the choice of interaction parameters as well as changes of the electronic structure through pressure. Our study uses a multi-orbital Hubbard model, incorporating all Ni  $3d$  and O  $2p$  states. We analyze the superconducting pairing mechanism of  $\text{La}_3\text{Ni}_2\text{O}_7$  within the random phase approximation and find a transition between  $d$ -wave and sign-changing  $s$ -wave pairing states as a function of pressure and interaction parameters, which is driven by spin-fluctuations with different wave vectors. Our work paves the way to understanding seemingly contradictory theoretical results within a unified framework.

*Introduction.*- The synthesis and physical properties of Ruddlesden-Popper nickelates have been studied for almost decades both in experiment [1] and theory [2]. Shortly after the initial synthesis of  $\text{La}_3\text{Ni}_2\text{O}_7$ , a metal-insulator transition in oxygen-deficient samples of  $\text{La}_3\text{Ni}_2\text{O}_{7-\delta}$  was discovered [3]. After the discovery of high- $T_c$  superconducting cuprates with  $\text{Cu}^{2+}$  ions (in  $3d^9$  configuration), interest in nickelates with  $\text{Ni}^{1+}$  (in  $3d^1$  configuration) also increased, since the community expected these compounds to mirror the properties of the cuprates [4]. Superconductivity in these materials, however, remained elusive until the discovery of superconducting thin-films of the infinite-layer nickelate  $\text{Nd}_{0.8}\text{Sr}_{0.2}\text{NiO}_2$  with a  $T_c$  of around 9 to 15 K [5]. In 2023, a significant breakthrough was achieved with the discovery of superconductivity in Ruddlesden-Popper phase bilayer nickelate  $\text{La}_3\text{Ni}_2\text{O}_7$  under a pressure of 14 GPa with a relatively high transition temperature of around 80 K [6].

Naturally, this new high- $T_c$  superconductor has since attracted much interest. Methods for the synthesis of this compound have been significantly improved. The maximum superconducting volume now reaches 48% for samples of pristine  $\text{La}_3\text{Ni}_2\text{O}_7$  [7] and close to 100% for the praseodymium-substituted material  $\text{La}_2\text{PrNi}_2\text{O}_7$  [8]. The crystal structure of  $\text{La}_3\text{Ni}_2\text{O}_7$  under pressure has meanwhile been resolved using X-ray diffraction. The materials undergo a structural phase transition from  $Amam$  to  $Fmmm$  (orthorhombic) and finally to  $I4/mmm$  (tetragonal) as a function of pressure and temperature [7, 9]. The onset of superconductivity in the pressure range from 14 GPa to 90 GPa has been determined using resistivity measurements, which results in a phase-diagram with a superconducting dome that is very steep at the low-pressure end and falls off slowly towards higher pressures [7].

Several other experiments have been performed that give further insight into this fascinating class of materials. Electron energy-loss spectroscopy shows strong  $p$ - $d$  hybridization and underscores the importance of considering the role of oxygen  $2p$  orbitals [10]. Based on X-ray absorption spectra, it has been argued that  $\text{La}_3\text{Ni}_2\text{O}_7$  displays behavior similar to the Zhang-Rice singlet observed in cuprates [11]. Experiments such as nuclear magnetic resonance spectroscopy of the  $^{139}\text{La}$  nuclei [12], muon spin relaxation [13], inelastic neutron scattering [14] and resistance measurements [15] indicate the presence of magnetic excitations and potential density-wave-like transitions. However, no long-range magnetic order has been found in neutron diffraction and inelastic neutron scattering experiments down to a temperature of 10 K [14, 16]. In addition, angle-resolved photoemission spectroscopy has mapped the Fermi surface and electronic band structure [17], which is a helpful guide for theoretical studies.

Since  $\text{La}_3\text{Ni}_2\text{O}_7$  shares some physical properties with cuprates, it is natural to ask whether the superconducting pairing mechanism and its symmetry also resemble those of high- $T_c$  cuprates. This question has been investigated using different theoretical methods, such as mean-field theory [19–22], random phase approximation (RPA) [23–26], fluctuation-exchange approximation [27], and functional renormalization group calculations [28–30]. Unfortunately, different studies yield different symmetries of the superconducting pairing, even if they use the same numerical method. However, it has been pointed out that the superconducting pairing symmetry of  $\text{La}_3\text{Ni}_2\text{O}_7$  is sensitive, e.g. to the crystal field splitting between the Ni  $e_g$  orbitals [31].

Previous studies use strongly downfolded few-orbital models, which are questionable in the presence of strong  $p$ - $d$  hybridization, and often retain only short range terms

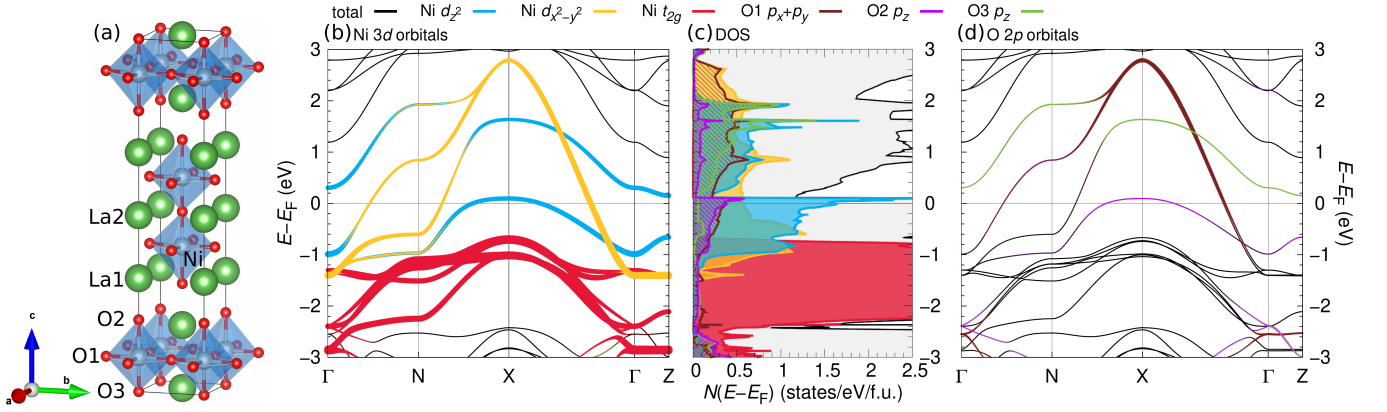


FIG. 1. Crystal structure, electronic band structure and density of states of  $\text{La}_3\text{Ni}_2\text{O}_7$ . (a) Crystal structure of  $\text{La}_3\text{Ni}_2\text{O}_7$  (space group  $I4/mmm$ , No. 139) with corner sharing  $\text{NiO}_6$  octahedra and marked labels of atoms for different Wyckoff positions. O1, O2, and O3 denote the inner-layer oxygen, apical oxygen, and inter-layer oxygen respectively. (b) Band structure of  $\text{La}_3\text{Ni}_2\text{O}_7$  with orbital weights of Ni 3d orbitals. (c) Orbital-resolved electronic density of states of  $\text{La}_3\text{Ni}_2\text{O}_7$ . (d) Orbital weights of the relevant subset of O 2p states. For the high symmetry points  $\Gamma = (0, 0, 0)$ ,  $N = (0, 1/2, 0)$ ,  $X = (0, 0, 1/2)$  and  $Z = (1/2, 1/2, -1/2)$  in terms of primitive reciprocal lattice vectors, we follow the rule of Ref. [18].

of the kinetic Hamiltonian. We go beyond these works by using a multi-orbital tight-binding model with all relevant orbitals in a wide energy window around the Fermi level. Our further calculations show that  $\text{La}_3\text{Ni}_2\text{O}_7$  hosts spin fluctuations of comparable strength with several different wave vectors, leading to a complex competition of possible pairing states. Additionally, we find that the choice of Hubbard interaction parameters can also modify the superconducting pairing symmetry. Our approach provides a framework for understanding the contradictory results reported in previous studies.

*Methods.*— We perform the density functional theory (DFT) calculation by using the full potential local orbital (FPLO) basis set [32] and using the generalized gradient approximation (GGA) to the exchange and correlation potential [33]. Our calculations are based on high-pressure experimental crystal structures of  $\text{La}_3\text{Ni}_2\text{O}_7$  [9] in space group  $I4/mmm$  (No. 139), for which we optimized the internal atomic positions within DFT.

Using projective Wannier functions as implemented in FPLO [34], we obtain tight-binding models that include all 31 orbitals with Ni 3d and O 2p character. In particular, we also retain small-valued and long-range transfer integrals, which results in the near-perfect reproduction of the three-dimensional DFT band energies. Due to the inclusion of oxygen 2p states we are also able to retain the relative orbital weights near the Fermi level with respect to the DFT results, which will be important when calculating the spin susceptibilities at a later stage. A comparison between the DFT bands and our 31 band tight binding model can be found in the supplementary material.

The kinetic part of the Hamiltonian can be written as:

$$H_0 = - \sum_{i,j,\sigma} t_{ij}^{sp} c_{is\sigma}^\dagger c_{jp\sigma}, \quad (1)$$

where  $t_{ij}^{sp}$  are the transfer integrals between sites  $i$  and  $j$ ,  $s$  and  $p$  are orbital indices, and  $\sigma$  is the spin index. Based on the tight-binding models, we calculate the non-interacting susceptibilities  $\chi_{st}^{pq}(\mathbf{q})$  [35].

We investigate the superconducting pairing due to spin fluctuations in  $\text{La}_3\text{Ni}_2\text{O}_7$  by adding a multi-orbital Hubbard interaction to our kinetic Hamiltonian [35]:

$$H = H_0 + U \sum_{i,l} n_{il\uparrow} n_{il\downarrow} + \frac{U'}{2} \sum_{i,s,p \neq s} n_{is} n_{ip} - \frac{J}{2} \sum_{i,s,p \neq s} \mathbf{S}_{is} \cdot \mathbf{S}_{ip} + \frac{J'}{2} \sum_{i,s,p \neq s,\sigma} c_{is\sigma}^\dagger c_{is\bar{\sigma}}^\dagger c_{ip\bar{\sigma}} c_{ip\sigma} \quad (2)$$

Here,  $c_{is\sigma}^\dagger$  ( $c_{is\sigma}$ ) denote fermionic creation (annihilation) operators,  $\mathbf{S}_{is}$  is the spin operator and  $n_{is\sigma} = c_{is\sigma}^\dagger c_{is\sigma}$  is the particle number operator. The interaction parameters are intra-orbital Coulomb repulsion  $U$ , inter-orbital Coulomb repulsion  $U'$ , Hund's rule coupling  $J$ , and pair hopping  $J'$ , which are applied to the Ni 3d orbitals and follow the Hubbard-Kanamori relation with  $U' = U - 2J$  and  $J' = J$  [36, 37].

We employ the multi-orbital random phase approximation [35, 38], which has delivered reliable results for cuprates [39], iron-based materials [40–42], and organic superconductors [43–45], to calculate the spin susceptibility and the symmetry of the superconducting pairing within a linearized Eliashberg approach [35]. This allows us to investigate competing pairing instabilities, for

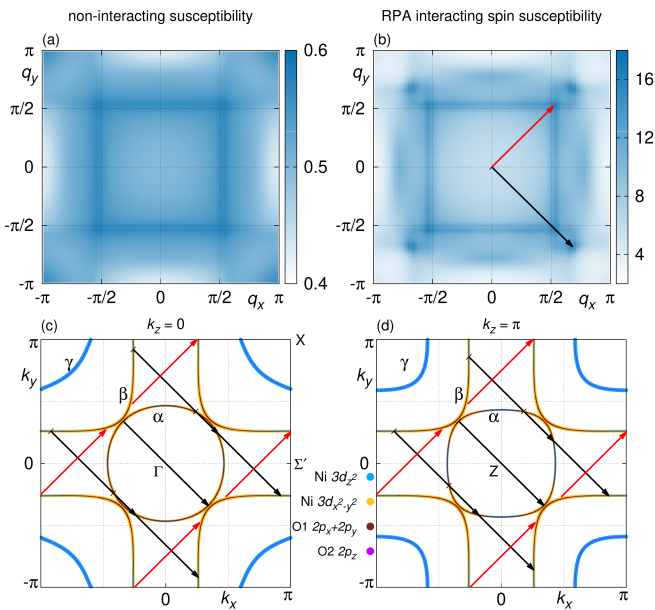


FIG. 2. Two-dimensional susceptibilities and Fermi surface with nesting vectors for  $\text{La}_3\text{Ni}_2\text{O}_7$  at a pressure of  $P = 24.6$  GPa. (a) Non-interacting susceptibility  $\chi_0$ . (b) RPA interacting spin susceptibility  $\chi_s$  for  $U = 3$  eV and  $J = 0.75$  eV. (c) Fermi surface at  $k_z = 0$ . (d) Fermi surface at  $k_z = \pi$ .

which we can obtain the superconducting gap function on the Fermi surface and the corresponding eigenvalue of the linearized Eliashberg equation, which is a measure of the pairing strength. To reduce the computational effort to a manageable level, we calculate susceptibilities and pairing only between Ni  $3d$  orbitals. We have previously used this approach for multi-orbital models of other materials [46].

*Results and Discussion.*— We start by investigating the crystal structure and electronic properties of  $\text{La}_3\text{Ni}_2\text{O}_7$ . In Fig. 1(a) we show the crystal structure of  $\text{La}_3\text{Ni}_2\text{O}_7$  with corner sharing  $\text{NiO}_6$  octahedra, and label different atoms with different Wyckoff positions to identify their contributions separately. Obviously, the oxygen orbitals not only connect the Ni-O plane, but also the bilayered Ni structure with the rest of the system. Due to the bilayered structure, oxygen plays a more important role in nickelates than in cuprates, which is also underscored by the strong hybridization between the O and Ni states and the experimental consequences of oxygen deficiency [3, 10, 11].

In Fig. 1(b), (c), and (d), we analyze the electronic band structure and density of states (DOS) of  $\text{La}_3\text{Ni}_2\text{O}_7$ . We identify the Ni  $3d$  orbitals with corresponding weights in Fig. 1(b) and the relevant orbitals of three different O positions in Fig. 1(d). Clearly, the Ni  $3d_{z^2}$  and  $3d_{x^2-y^2}$  orbitals dominate at the Fermi level, but the presence of O  $2p$  orbitals is not weak enough to be neglected. This is also evident in the electronic DOS shown in Fig. 1(c). We find that largest relative orbital-resolved contributions to

the DOS at the Fermi level  $N(E_F)$  are 47.6% (Ni  $3d_{z^2}$ ), 17.6% (Ni  $3d_{x^2-y^2}$ ), 11.3% (O1  $2p_x + 2p_y$ ), and 10.8% (O2  $2p_z$ ). We now focus on the contributions from these orbitals, since the other orbitals each contribute less than 2%. Although the Fermi level is dominated by Ni  $3d_{z^2}$  and  $3d_{x^2-y^2}$  orbitals, the oxygen  $2p_x$  and  $2p_y$  of the O1 position inside the Ni-O plane is almost as important as the Ni  $3d_{x^2-y^2}$  orbital. The relevance of these orbitals is obvious from the crystal geometry, since they point directly towards the Ni atoms within the plane.

The large contribution from the oxygen  $2p_z$  orbitals on the O2 position, which are perpendicular to the Ni-O plane, is somewhat surprising and has not been previously considered. Most importantly, this orbital (see Fig. 1(d)) together with the Ni  $3d_{z^2}$  orbital (see Fig. 1(b)) is responsible for the hole pocket around the X-point. About one fifth of the weight on the  $\gamma$  Fermi surface (see Fig. 2(c) and (d)) is contributed by oxygen  $2p_z$  states, while the rest can be attributed to Ni  $3d_{z^2}$  states. Therefore, it is evident that models for  $\text{La}_3\text{Ni}_2\text{O}_7$  need to consider at least these oxygen orbitals in addition to the Ni  $e_g$  states to correctly capture the physics close to the Fermi surface.

The non-interacting susceptibility  $\chi_0$  (see Fig. 2(a)) calculated from our 31 band model is a first indication of the momentum structure of spin fluctuations, which result from nesting of the Fermi surface. Note that we fully take into account the matrix elements between all involved orbitals when calculating this susceptibility, which goes far beyond simple Fermi surface nesting. We now use RPA for the multi-orbital Hubbard Hamiltonian (see eq. 2) to calculate the static spin susceptibility  $\chi_s$ , i.e. the spin fluctuations on the Fermi surface. The spin susceptibility for pressure  $P = 24.6$  GPa and interaction parameters  $U = 3$  eV and  $J = 0.75$  eV is shown in Fig. 2(b).

In Fig. 2(c) and (d) we show the orbital weights on the Fermi surface in the  $k_x$ - $k_y$ -plane at  $k_z = 0$  and  $k_z = \pi$ , respectively. Based on our interacting susceptibility shown in Fig. 2(b) we identified the most important nesting vectors, from which superconductivity driven by spin fluctuations may result. While the non-interacting susceptibility shows a strong peak at  $\mathbf{q} \sim (\pi/2, \pi/2)$ , other momentum vectors are more strongly enhanced by interactions in the spin susceptibility. In particular, at  $\mathbf{q} \sim (7\pi/10, 7\pi/10)$  a strong peak emerges (see Fig. 2(b)). Furthermore, we observe a square-shaped structure of continuously large spin susceptibility, with strong peaks at its corners with momentum  $\mathbf{q} = (\pi/2, \pi/2)$ . The well-known connection between magnetic instabilities and spin susceptibility suggests that magnetism in  $\text{La}_3\text{Ni}_2\text{O}_7$  could be somewhat frustrated by the incompatible wave vectors of spin fluctuations with comparable intensity. In other words, the spin fluctuations at  $\mathbf{q} \sim (\pi/2, \pi/2)$  and  $\mathbf{q} \sim (7\pi/10, 7\pi/10)$  are incompatible when it comes to magnetic ordering, but may both contribute to superconducting pairing in  $\text{La}_3\text{Ni}_2\text{O}_7$ . Such a magnetic frus-

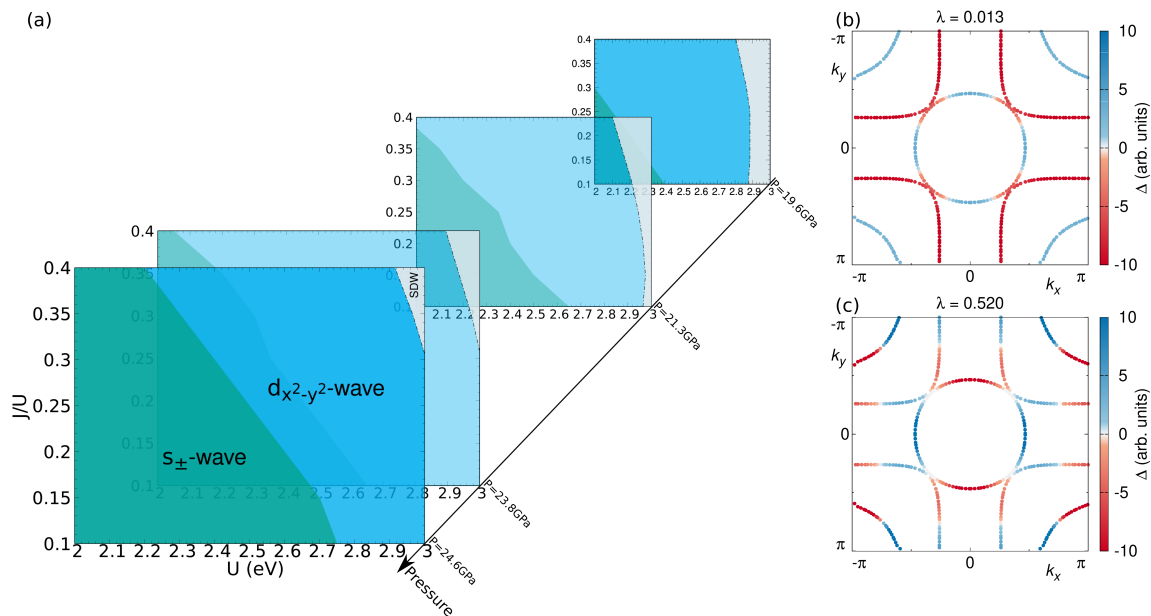


FIG. 3. (a) Phase diagram of the superconducting pairing symmetry of  $\text{La}_3\text{Ni}_2\text{O}_7$  as a function of pressure and interaction parameters  $U$  and  $J$ . (b) Typical sign-changing  $s$ -wave superconducting gap (at  $U = 2$  eV,  $J = 0.5$  eV and  $P = 24.6$  GPa). (c) Typical  $d_{x^2-y^2}$ -wave superconducting gap ( $U = 3$  eV,  $J = 0.75$  eV and  $P = 24.6$  GPa).

tration has previously been identified as an important property of iron chalcogenides [47] and deserves further study for the nickelate family of materials.

Previous RPA studies have mostly reported a superconducting gap function of sign-changing ( $s_{\pm}$ ) type [23, 24], while a minority reported  $d$ -wave pairing [25]. The mechanism behind the appearance of both order parameters in calculations was partially explained by tuning the crystal field splitting [31]. However, all previous studies have used few-orbital models with unrealistically small interaction parameters  $U$  and  $J$ , which deviate from the common understanding of  $3d$  electron systems and also the theoretical values obtained from constrained RPA calculations [48].

However, almost all previous studies use few-orbital models with small  $U$  and  $J$  that are far from the common understanding of  $3d$  electron system and also the prediction of constrained RPA calculations [48]. The reason for these discrepancies is rather obvious from our electronic band structure. In a few-orbital model, the weight of missing orbitals compared to DFT is arbitrarily replaced by weights of the included orbitals, which leads to the underestimation of critical interaction values for the  $d$  electrons and alters the momentum structure of resulting susceptibilities. Since we have found that various oxygen orbitals have important contributions on the Fermi surface of  $\text{La}_3\text{Ni}_2\text{O}_7$  and are very differentiated in momentum space, neglecting them will also inevitably falsify the results of any spin fluctuation pairing calculation.

We now investigate the superconducting pairing of

$\text{La}_3\text{Ni}_2\text{O}_7$  based on realistic three-dimensional multi-orbital models based on crystal structures at four different pressures [9] within RPA. We calculate the symmetry of the leading superconducting pairing instability as a function of pressure, intra-orbital Coulomb interaction  $U$  and Hund's rule coupling  $J$ . Our results in Fig. 3(a) show that the superconducting pairing symmetry is sensitive to both pressure and the relative size of interaction parameters. Our phase diagram contains a previously overlooked transition between  $s_{\pm}$ - and  $d$ -wave order parameters, which results from the competition of spin fluctuations with different wave vectors. Both modifications of the electronic structure and a change in interaction parameters tune this competition and can lead to different leading symmetries of the superconducting pairing. Therefore, we believe that previous studies correspond to a specific combination of the parameters, which are incidentally located on different sides of the phase transition found in our study.

As an example, we discuss the superconducting pairing symmetry for the  $P = 24.6$  GPa case (leftmost in Fig. 3(a)). For small interaction values, the sign-changing  $s$ -wave ( $s_{\pm}$ ) pairing leads, while increasing  $U$  changes the dominant pairing to  $d_{x^2-y^2}$  symmetry. Increasing the Hund's rule coupling also changes the order parameter from  $s_{\pm}$  to  $d_{x^2-y^2}$ . Note that our phase diagram also contains areas, where the spin susceptibility diverges and the RPA becomes unstable. We identify these regions with potential spin-density wave states, denoted as SDW in our phase diagram. Moreover, we find that increasing pressure enlarges the are of the phase di-



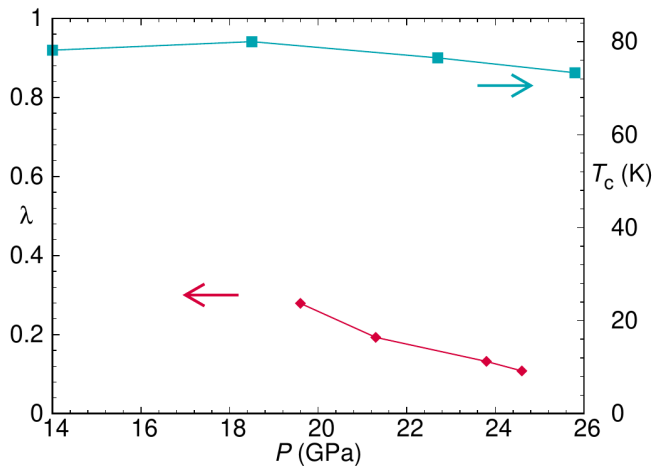


FIG. 4. Leading eigenvalues  $\lambda$  of the superconducting gap function as a function of pressure at  $U = 2.8$  eV,  $J = 0.7$  eV.  $T_c^{\text{onset}}$  data are from Ref. [6].

agram covered by the  $s_{\pm}$  state, i.e. the  $d_{x^2-y^2}$ -wave pairing phase is shifted to higher values of the intra-orbital Coulomb interaction  $U$ .

The evolution of the electronic band structure with increasing pressure shown in the supplementary material reveals that pressure directly tunes the crystal field splitting. With increasing pressure, the crystal field splitting becomes larger and the  $s_{\pm}$ -wave pairing is enhanced (see Fig. 3(a)). Therefore, our results also contain the effect of crystal field splitting on the superconducting pairing, which was previously observed in Ref. [31].

Furthermore, we observe that the instability of RPA moves to higher interaction parameters with increasing pressure, which signals a decrease in the strength of spin-fluctuations, i.e. increasing pressure moves  $\text{La}_3\text{Ni}_2\text{O}_7$  farther away from magnetic ordering. This observation is also consistent with the peculiar shape of the superconducting dome [7], where high  $T_c$  is located at the low-pressure side of the dome.

In Fig. 3(b) and (c), we show examples of  $s_{\pm}$ - and  $d_{x^2-y^2}$ -wave gap functions on the Fermi surface at  $P = 24.6$  GPa. We chose  $U = 2$  eV,  $J = 0.5$  eV and  $U = 3$  eV,  $J = 0.75$  eV, respectively. Note that the  $d_{x^2-y^2}$ -wave state contains additional sign changes due to the presence of sub-leading nesting vectors. From the sign-changes of the superconducting gap it is clear that the  $d_{x^2-y^2}$ -wave state is mainly driven by the  $\mathbf{q} \sim (7\pi/10, 7\pi/10)$  nesting vector, while  $\mathbf{q} = (\pi/2, \pi/2)$  drives the additional sign-change of the  $d_{x^2-y^2}$ -wave state as well as the sign-changing  $s$ -wave state.

We also calculated the eigenvalue  $\lambda$  of the linearized Eliashberg equation as a function of pressure, which may serve as a measure of the strength of pairing via spin-fluctuations. In Fig. 4 we show that the theoretically calculated pairing strength shows a moderate decrease in the investigated pressure region. This behavior is rem-

iniscent of the high-pressure region ( $P > 18$  GPa) of the superconducting dome in  $\text{La}_3\text{Ni}_2\text{O}_7$  [6, 7], which also shows a slow decrease of  $T_c$  with pressure. Thus, our findings based on a spin-fluctuation pairing mechanism are clearly consistent with the experimental properties of the tetragonal  $I4/mmm$  phase of  $\text{La}_3\text{Ni}_2\text{O}_7$ .

*Conclusions.*- We have shown that the symmetry of the superconducting gap in multi-orbital Hubbard models for  $\text{La}_3\text{Ni}_2\text{O}_7$  is sensitive to pressure, the value of Coulomb interaction  $U$  and the Hund's rule coupling  $J$ . We have also shown that pressure directly tunes the crystal field splitting between the Ni  $e_g$  orbitals, while reducing the strength of the superconducting pairing, both in agreement with previous reports [7, 31].

In our models we found  $s_{\pm}$ - as well as  $d_{x^2-y^2}$ -wave pairing symmetries depending on crystal field splitting and interaction parameters. In particular, our results in the  $s_{\pm}$ -phase (for low Coulomb interaction  $U$ ) reproduce the results of few-orbital models reported in the literature. In addition, we discovered a transition to a  $d_{x^2-y^2}$ -wave state, which was also reported in the literature, upon increasing the interaction parameters  $U$  and  $J$ . Therefore, our multi-orbital approach to superconductivity in  $\text{La}_3\text{Ni}_2\text{O}_7$  provides a unified framework for understanding a large number of experimental and seemingly inconsistent theoretical results.

While the reductionist idea behind few-orbital models certainly has its merits, materials with strong hybridization such as  $\text{La}_3\text{Ni}_2\text{O}_7$  sometimes make it necessary to go beyond minimal models. We have shown that a model for  $\text{La}_3\text{Ni}_2\text{O}_7$  at least needs to include the Ni  $3d_{z^2}$ , Ni  $3d_{x^2-y^2}$ , O1  $2p_x + 2p_y$  and O2  $2p_z$ . Further reduction of the number of orbitals leads to the arbitrary redistribution of orbital weights near the Fermi surface, which alters the momentum structure of spin fluctuations and lowers critical interactions to unrealistic values.

Based on our findings, it seems possible that  $\text{La}_3\text{Ni}_2\text{O}_7$  can be tuned from a  $d_{x^2-y^2}$ -wave state towards a sign-changing  $s$ -wave state by application of pressure or another technique that can manipulate the crystal field splitting between Ni  $e_g$  orbitals and/or the strength of interactions.

We acknowledge fruitful discussions with Ningning Wang for his explanation of experiments. We are thankful for the useful discussions with Xianxin Wu, Hanghui Chen, Qiang-Hua Wang, Meng Wang in IOP conferences and lectures, and revealing questions from Changming Yue, Karsten Held, Nayuta Takemori, Masao Ogata, in CCMP 2024. This work was supported by the National Natural Science Foundation of China (Grants No. 12188101), National Key R&D Program of China (Grants No. 2022YFA1403800, No. 2024YFA1408400), and the Center for Materials Genome.

- [1] Z. Zhang, M. Greenblatt, and J. Goodenough, Synthesis, structure, and properties of the layered perovskite  $\text{La}_3\text{Ni}_2\text{O}_{7-\delta}$ , *J. Solid State Chem.* **108**, 402 (1994).
- [2] D.-K. Seo, W. Liang, M.-H. Whangbo, Z. Zhang, and M. Greenblatt, Electronic band structure and Madelung potential study of the nickelates  $\text{La}_2\text{NiO}_4$ ,  $\text{La}_3\text{Ni}_2\text{O}_7$ , and  $\text{La}_4\text{Ni}_3\text{O}_{10}$ , *Inorg. Chem.* **35**, 6396 (1996).
- [3] S. Taniguchi, T. Nishikawa, Y. Yasui, Y. Kobayashi, J. Takeda, S.-i. Shamoto, and M. Sato, Transport, magnetic and thermal properties of  $\text{La}_3\text{Ni}_2\text{O}_{7-\delta}$ , *J. Phys. Soc. Jpn.* **64**, 1644 (1995).
- [4] M. Hayward, M. Green, M. Rosseinsky, and J. Sloan, Sodium hydride as a powerful reducing agent for topotactic oxide deintercalation: synthesis and characterization of the nickel (I) oxide  $\text{LaNiO}_2$ , *J. Am. Chem. Soc.* **121**, 8843 (1999).
- [5] D. Li, K. Lee, B. Y. Wang, M. Osada, S. Crossley, H. R. Lee, Y. Cui, Y. Hikita, and H. Y. Hwang, Superconductivity in an infinite-layer nickelate, *Nature* **572**, 624 (2019).
- [6] H. Sun, M. Huo, X. Hu, J. Li, Z. Liu, Y. Han, L. Tang, Z. Mao, P. Yang, B. Wang, *et al.*, Signatures of superconductivity near 80 K in a nickelate under high pressure, *Nature* **621**, 493 (2023).
- [7] J. Li, P. Ma, H. Zhang, X. Huang, C. Huang, M. Huo, D. Hu, Z. Dong, C. He, J. Liao, *et al.*, Pressure-driven dome-shaped superconductivity in bilayer nickelate  $\text{La}_3\text{Ni}_2\text{O}_7$  (2024), [arXiv:2404.11369](https://arxiv.org/abs/2404.11369).
- [8] N. Wang, G. Wang, X. Shen, J. Hou, J. Luo, X. Ma, H. Yang, L. Shi, J. Dou, J. Feng, *et al.*, Bulk high-temperature superconductivity in pressurized tetragonal  $\text{La}_2\text{PrNi}_2\text{O}_7$ , *Nature* **634**, 579 (2024).
- [9] L. Wang, Y. Li, S.-Y. Xie, F. Liu, H. Sun, C. Huang, Y. Gao, T. Nakagawa, B. Fu, B. Dong, Z. Cao, R. Yu, S. I. Kawaguchi, H. Kadobayashi, M. Wang, C. Jin, H.-k. Mao, and H. Liu, Structure responsible for the superconducting state in  $\text{La}_3\text{Ni}_2\text{O}_7$  at high-pressure and low-temperature conditions, *J. Am. Chem. Soc.* **146**, 7506 (2024).
- [10] Z. Dong, M. Huo, J. Li, J. Li, P. Li, H. Sun, L. Gu, Y. Lu, M. Wang, Y. Wang, *et al.*, Visualization of oxygen vacancies and self-doped ligand holes in  $\text{La}_3\text{Ni}_2\text{O}_{7-\delta}$ , *Nature* **630**, 847 (2024).
- [11] X. Ren, R. Sutarto, X. Wu, J. Zhang, H. Huang, T. Xiang, J. Hu, R. Comin, X. Zhou, and Z. Zhu, Resolving the electronic ground state of  $\text{La}_3\text{Ni}_2\text{O}_{7-\delta}$  films (2024), [arXiv:2409.04121](https://arxiv.org/abs/2409.04121).
- [12] Z. Dan, Y. Zhou, M. Huo, Y. Wang, L. Nie, M. Wang, T. Wu, and X. Chen, Spin-density-wave transition in double-layer nickelate  $\text{La}_3\text{Ni}_2\text{O}_7$  (2024), [arXiv:2402.03952](https://arxiv.org/abs/2402.03952).
- [13] K. Chen, X. Liu, J. Jiao, M. Zou, C. Jiang, X. Li, Y. Luo, Q. Wu, N. Zhang, Y. Guo, *et al.*, Evidence of spin density waves in  $\text{La}_3\text{Ni}_2\text{O}_{7-\delta}$ , *Phys. Rev. Lett.* **132**, 256503 (2024).
- [14] T. Xie, M. Huo, X. Ni, F. Shen, X. Huang, H. Sun, H. C. Walker, D. Adroja, D. Yu, B. Shen, *et al.*, Neutron scattering studies on the high- $T_c$  superconductor  $\text{La}_3\text{Ni}_2\text{O}_{7-\delta}$  at ambient pressure (2024), [arXiv:2401.12635](https://arxiv.org/abs/2401.12635).
- [15] Y. Zhang, D. Su, Y. Huang, Z. Shan, H. Sun, M. Huo, K. Ye, J. Zhang, Z. Yang, Y. Xu, *et al.*, High-temperature superconductivity with zero resistance and strange-metal behaviour in  $\text{La}_3\text{Ni}_2\text{O}_{7-\delta}$ , *Nat. Phys.* **20**, 1269 (2024).
- [16] C. D. Ling, D. N. Argyriou, G. Wu, and J. Neumeier, Neutron diffraction study of  $\text{La}_3\text{Ni}_2\text{O}_7$ : Structural relationships among  $n = 1, 2$ , and 3 phases  $\text{La}_{n+1}\text{Ni}_n\text{O}_{3n+1}$ , *J. Solid State Chem.* **152**, 517 (2000).
- [17] J. Yang, H. Sun, X. Hu, Y. Xie, T. Miao, H. Luo, H. Chen, B. Liang, W. Zhu, G. Qu, *et al.*, Orbital-dependent electron correlation in double-layer nickelate  $\text{La}_3\text{Ni}_2\text{O}_7$ , *Nat. Commun.* **15**, 4373 (2024).
- [18] W. Setyawan and S. Curtarolo, High-throughput electronic band structure calculations: Challenges and tools, *Comput. Mater. Sci.* **49**, 299 (2010).
- [19] Y. Gu, C. Le, Z. Yang, X. Wu, and J. Hu, Effective model and pairing tendency in bilayer Ni-based superconductor  $\text{La}_3\text{Ni}_2\text{O}_7$  (2023), [arXiv:2306.07275](https://arxiv.org/abs/2306.07275).
- [20] K. Jiang, Z. Wang, and F.-C. Zhang, High-temperature superconductivity in  $\text{La}_3\text{Ni}_2\text{O}_7$ , *Chin. Phys. Lett.* **41**, 017402 (2024).
- [21] Z. Luo, B. Lv, M. Wang, W. Wú, and D.-X. Yao, High- $T_c$  superconductivity in  $\text{La}_3\text{Ni}_2\text{O}_7$  based on the bilayer two-orbital t-J model, *npj Quantum Mater.* **9**, 61 (2024).
- [22] C. Lu, Z. Pan, F. Yang, and C. Wu, Interlayer-coupling-driven high-temperature superconductivity in  $\text{La}_3\text{Ni}_2\text{O}_7$  under pressure, *Phys. Rev. Lett.* **132**, 146002 (2024).
- [23] Y. Zhang, L.-F. Lin, A. Moreo, T. A. Maier, and E. Dagotto, Structural phase transition,  $s_{\pm}$ -wave pairing, and magnetic stripe order in bilayered superconductor  $\text{La}_3\text{Ni}_2\text{O}_7$  under pressure, *Nat. Commun.* **15**, 2470 (2024).
- [24] S. Bötzel, F. Lechermann, J. Gondolf, and I. M. Eremin, Theory of magnetic excitations in the multilayer nickelate superconductor  $\text{La}_3\text{Ni}_2\text{O}_7$ , *Phys. Rev. B* **109**, L180502 (2024).
- [25] F. Lechermann, J. Gondolf, S. Bötzel, and I. M. Eremin, Electronic correlations and superconducting instability in  $\text{La}_3\text{Ni}_2\text{O}_7$  under high pressure, *Phys. Rev. B* **108**, L201121 (2023).
- [26] Y.-B. Liu, J.-W. Mei, F. Ye, W.-Q. Chen, and F. Yang,  $s_{\pm}$ -wave pairing and the destructive role of apical-oxygen deficiencies in  $\text{La}_3\text{Ni}_2\text{O}_7$  under pressure, *Phys. Rev. Lett.* **131**, 236002 (2023).
- [27] G. Heier, K. Park, and S. Y. Savrasov, Competing  $d_{xy}$  and  $s_{\pm}$  pairing symmetries in superconducting  $\text{La}_3\text{Ni}_2\text{O}_7$ : LDA + FLEX calculations, *Phys. Rev. B* **109**, 104508 (2024).
- [28] Q.-G. Yang, D. Wang, and Q.-H. Wang, Possible  $s_{\pm}$ -wave superconductivity in  $\text{La}_3\text{Ni}_2\text{O}_7$ , *Phys. Rev. B* **108**, L140505 (2023).
- [29] K.-Y. Jiang, Y.-H. Cao, Q.-G. Yang, H.-Y. Lu, and Q.-H. Wang, Theory of pressure dependence of superconductivity in bilayer nickelate  $\text{La}_3\text{Ni}_2\text{O}_7$  (2024), [arXiv:2409.17861](https://arxiv.org/abs/2409.17861).
- [30] J. Zhan, Y. Gu, X. Wu, and J. Hu, Cooperation between electron-phonon coupling and electronic interaction in bilayer nickelates  $\text{La}_3\text{Ni}_2\text{O}_7$  (2024), [arXiv:2404.03638](https://arxiv.org/abs/2404.03638).
- [31] H. Liu, C. Xia, S. Zhou, and H. Chen, Role of crystal-field-splitting and long-range-hoppings on superconducting pairing symmetry of  $\text{La}_3\text{Ni}_2\text{O}_7$  (2023), [arXiv:2311.07316](https://arxiv.org/abs/2311.07316).
- [32] K. Koepnick and H. Eschrig, Full-potential nonorthogonal local-orbital minimum-basis band-structure scheme, *Phys. Rev. B* **59**, 1743 (1999).
- [33] J. P. Perdew, K. Burke, and M. Ernzerhof, Generalized

- gradient approximation made simple, *Phys. Rev. Lett.* **77**, 3865 (1996).
- [34] H. Eschrig and K. Koepernik, Tight-binding models for the iron-based superconductors, *Phys. Rev. B* **80**, 104503 (2009).
- [35] S. Graser, T. A. Maier, P. J. Hirschfeld, and D. J. Scalapino, Near-degeneracy of several pairing channels in multiorbital models for the Fe pnictides, *New J. Phys.* **11**, 025016 (2009).
- [36] J. Kanamori, Electron correlation and ferromagnetism of transition metals, *Prog. Theor. Phys.* **30**, 275 (1963).
- [37] A. Georges, L. d. Medici, and J. Mravlje, Strong correlations from Hund's coupling, *Annu. Rev. Condens. Matter Phys.* **4**, 137 (2013).
- [38] M. Altmeyer, D. Guterding, P. J. Hirschfeld, T. A. Maier, R. Valentí, and D. J. Scalapino, Role of vertex corrections in the matrix formulation of the random phase approximation for the multiorbital Hubbard model, *Phys. Rev. B* **94**, 214515 (2016).
- [39] M. Roig, A. T. Rømer, P. J. Hirschfeld, and B. M. Andersen, Revisiting superconductivity in the extended one-band Hubbard model: Pairing via spin and charge fluctuations, *Phys. Rev. B* **106**, 214530 (2022).
- [40] K. Suzuki, H. Usui, K. Kuroki, S. Iimura, Y. Sato, S. Matsuishi, and H. Hosono, Robust spin fluctuations and  $s\pm$  pairing in the heavily electron doped iron-based superconductors, *J. Phys. Soc. Jpn.* **82**, 083702 (2013).
- [41] A. Kreisel, B. M. Andersen, P. O. Sprau, A. Kostin, J. C. S. Davis, and P. J. Hirschfeld, Orbital selective pairing and gap structures of iron-based superconductors, *Phys. Rev. B* **95**, 174504 (2017).
- [42] M. Shimizu, N. Takemori, D. Guterding, and H. O. Jeschke, Two-dome superconductivity in FeS induced by a Lifshitz transition, *Phys. Rev. Lett.* **121**, 137001 (2018).
- [43] H. Aizawa, K. Kuroki, S. Yasuzuka, and J. Yamada, Model construction and superconductivity analysis of organic conductors  $\beta$ -(BDA-TTP)<sub>2</sub>MF<sub>6</sub> (M = P, As, Sb and Ta) based on first-principles band calculation, *New J. Phys.* **14**, 113045 (2012).
- [44] D. Guterding, S. Diehl, M. Altmeyer, T. Methfessel, U. Tutsch, H. Schubert, M. Lang, J. Müller, M. Huth, H. O. Jeschke, R. Valentí, M. Jourdan, and H.-J. Elmers, Evidence for eight-node mixed-symmetry superconductivity in a correlated organic metal, *Phys. Rev. Lett.* **116**, 237001 (2016).
- [45] T. Mori, Low-symmetry gap functions of organic superconductors, *J. Phys. Soc. Jpn.* **87**, 044705 (2018).
- [46] H.-X. Xu, D. Guterding, and H. O. Jeschke, Theory for doping trends in titanium oxypnictide superconductors, *Phys. Rev. B* **104**, 184519 (2021).
- [47] J. Glasbrenner, I. Mazin, H. O. Jeschke, P. Hirschfeld, R. Fernandes, and R. Valentí, Effect of magnetic frustration on nematicity and superconductivity in iron chalcogenides, *Nat. Phys.* **11**, 953 (2015).
- [48] V. Christiansson, F. Petocchi, and P. Werner, Correlated electronic structure of La<sub>3</sub>Ni<sub>2</sub>O<sub>7</sub> under pressure, *Phys. Rev. Lett.* **131**, 206501 (2023).